

# RSC Advances



This is an *Accepted Manuscript*, which has been through the Royal Society of Chemistry peer review process and has been accepted for publication.

*Accepted Manuscripts* are published online shortly after acceptance, before technical editing, formatting and proof reading. Using this free service, authors can make their results available to the community, in citable form, before we publish the edited article. This *Accepted Manuscript* will be replaced by the edited, formatted and paginated article as soon as this is available.

You can find more information about *Accepted Manuscripts* in the [Information for Authors](#).

Please note that technical editing may introduce minor changes to the text and/or graphics, which may alter content. The journal's standard [Terms & Conditions](#) and the [Ethical guidelines](#) still apply. In no event shall the Royal Society of Chemistry be held responsible for any errors or omissions in this *Accepted Manuscript* or any consequences arising from the use of any information it contains.



## Assimilation of chitin with tin for defluoridation of water

A. Shekhawat,<sup>a</sup> S. S. Kahu,<sup>a</sup> D. Saravanan<sup>b</sup> and R. M. Jugade<sup>a</sup>

Received 00th January 20xx,  
Accepted 00th January 20xx

DOI: 10.1039/x0xx00000x

www.rsc.org/

Chitin, a natural amino polysaccharide, has been incorporated with Sn(VI) for effective adsorption of fluoride from water. The impregnation of Sn(VI) on chitin was carried out using microwave assisted technique. The material was thoroughly characterized using FTIR, SEM, EDX and XRD. The increase in surface area and pore volume as revealed by BET studies and enhanced thermal stability TGA-DTA studies have proved it to be a better adsorbent compared to chitin. This tin-impregnated chitin (SnC) has been exploited for its defluoridation property. Optimum working conditions include pH 4.0, adsorbent dose of 100 mg and contact time of 45 minutes. Under optimum conditions, SnC was found to have adsorption capacity of 14.77 mg/g. The equilibrium studies showed that the data fits well with Freundlich isotherm model. Thermodynamics and kinetics parameters have been evaluated. The material has been applied for the defluoridation of real water sample resulting in 95.6% fluoride removal in a single run. SnC was found to be recyclable material and can be regenerated and reused multiple times adding a greener dimension.

### Introduction

Fluoride contamination is a common problem in areas where ground water contains alarming concentrations of fluoride. WHO guidelines suggest 1 mg/L as the maximum permissible limit for drinking water<sup>1</sup>. Higher concentrations of fluoride are known to cause digestive, respiratory and nervous system disorders in addition to fluorosis<sup>2-4</sup>. Excess of fluoride has been reported to interfere in carbohydrate metabolism and damage DNA<sup>5</sup>.

Dissolution of mineral rocks and soils in water<sup>6</sup> and the waste water released from semiconductor industries, thermal power plants, electroplating, rubber and fertilizer industries are reasons for increased fluoride concentration in drinking water<sup>7</sup>. This is of great concern for more than 20 developed and developing countries. Fluorosis is endemic in China, India, Rift Valley countries in Africa and Sri Lanka. Therefore, it is important to develop effective methodologies for remediation of fluoride.

Defluoridation of ground water as well as effluents has always been a challenge. Ion exchange, precipitation, reverse osmosis and adsorption are the common defluoridation techniques<sup>8</sup>. Adsorption technique is cost effective, highly efficient as well as eco-friendly. Biosorbents like cellulose, chitin and chitosan have been used in native form or in modified form for defluoridation of water. Due to small size and high

electronegativity of fluorine, it has a great tendency to interact with multivalent metal ions and rare earth metals such as zirconium and lanthanum. Zr(IV)–ethylene diammine<sup>9</sup>, alginate entrapped Fe(III)–Zr(IV)<sup>10</sup>, zirconium impregnated collagen<sup>11</sup>, zirconium impregnated activated charcoal<sup>12</sup>, and lanthanum modified chitosan<sup>13</sup> are some of the sorbents reported for adsorption of fluoride. Biocompatibility and biodegradability of biopolymers make them effective host matrix for the incorporation of multivalent metal ions as compared to synthetic polymers<sup>14</sup>.

Chitin is the most abundant natural amino polysaccharide and is estimated to be produced annually almost as much as cellulose. It has become the material of great interest not only as an underutilized resource, but also as a new functional material of high potential in various fields. It has gained much attention for biomedical applications due to its biocompatibility and restorative properties. Its crystalline structure, resulting from intra- and intermolecular hydrogen bonds, is responsible to a great extent for its thermal and chemical stability<sup>15-17</sup>. However, its poor adsorption capability towards fluoride led to its non-applicability for defluoridation. In order to overcome this problem, modified chitin composites can be synthesized and such composites have been reported for fluoride removal<sup>18-20</sup>. Tin(IV), a cation with high positive charge, has been incorporated into the lattice structure of iron(III) oxide and used as an adsorbent for the removal of the fluoride ion from the aqueous phase<sup>21</sup>.

In present work, we report a novel compound formed by impregnation of tin metal on chitin biopolymer matrix. It has been applied for fluoride removal with better adsorption capacity as compared to reported modified biopolymers.

<sup>a</sup> Department of Chemistry, R.T.M. Nagpur University, Nagpur-440033, India

<sup>b</sup> Department of Chemistry, National College, Tiruchirappalli-620001, India.

† Footnotes relating to the title and/or authors should appear here.

Electronic Supplementary Information (ESI) available: [details of any supplementary information available should be included here]. See DOI: 10.1039/x0xx00000x

## Experimental

### Materials

Analytical grade reagents were used for the fluoride adsorption studies. Millipore water (Elix 3 Millipore unit) was used in preparation of the stock solution of fluoride. A 1000 mg/L stock solution of fluoride was prepared using sodium fluoride (Merck, India) and stored in a polypropylene bottle. The working solutions of 5, 10 and 15 mg/L fluoride were prepared by appropriate dilutions in polypropylene volumetric flasks. Chitin was procured from Loba Chemie Private Limited, India. All the chemicals were used as received without further purification.

### Preparation of Sn-impregnated chitin (SnC) adsorbent

A known weight of chitin biopolymer (2.0 g) was dispersed in minimum volume of acetone. About 2 mL of anhydrous Sn (IV) chloride was added to the dispersed chitin and stirred for 10 min to get a homogeneous mixture. It was subjected to microwave irradiation for 2 min with 30 s alternating time interval. It was filtered and washed with Millipore water till negative test of chloride was obtained. The SnC adsorbent was dried at 60 °C in a vacuum oven (Biotechnics, India) for 4 h. This solid material was characterized thoroughly and used for adsorption studies.

### Physico-chemical characterization

Structural details of Sn-chitin could be explained on the basis of FT-IR spectra recorded using Bruker *Alpha* spectrometer in the wavelength range 500-4000 cm<sup>-1</sup>. The XRD spectra were recorded by X-ray diffractometer system Righaku-Miniflex 300. Surface morphology of adsorbent was studied using Scanning Electron Microscope (SEM) model TESCAN VEGA 3 SBH. Energy dispersive X-ray (EDX) analysis was performed for elemental composition using X-ray analyzer Oxford INCA Energy 250 EDS System during SEM studies. Thermal analysis of SnC was carried out using Setsvs TG-DTA 16. The Brunauer–Emmet–Teller (BET) surface area estimation was carried out by nitrogen adsorption–desorption method on single point surface area analyzer model Smart Sorb 92/93.

### Analysis

The concentration of fluoride was measured using ORION pH/ISE meter 710 At equipped with a calibrated fluoride ion electrode model ORION 9609 BNWP. The reproducibility of instrument was checked by using TISAB II buffer. Calibration of fluoride ion selective electrode was performed by using 1, 5 and 10 mg/L standard solutions of fluoride which gave an optimum slope between 90 and 100%.

### Adsorption procedure

For batch adsorption studies, 5-70 mg/L fluoride solutions was equilibrated with 100 mg SnC in a stoppered polypropylene conical flasks. Each system was stirred for 45 min. The amount

of fluoride adsorbed (mg /g) on SnC at equilibrium ( $q_e$ ) can be given by-

$$q_e = \frac{C_0 - C_e}{W} \times V \quad (1)$$

also the percent removal capacity was calculated using following formula.

$$\% \text{Removal} = \frac{C_0 - C_e}{C_0} \times 100 \quad (2)$$

where  $C_0$  and  $C_e$  refer to the initial and equilibrium liquid phase concentrations in mg /L of fluoride,  $V$  is the volume of fluoride solution in liter and  $W$  is the weight of SnC adsorbent in gram. All the batch adsorption experiments were performed with three replicates to obtain reliable results.

## Results and discussion

### Material Characterization

In the FTIR spectrum of pure chitin (Fig.1a), the bands at 3452 and 3266 cm<sup>-1</sup> can be attributed to the -OH and -NH stretching respectively. The bands ranging from 2886 to 2961 cm<sup>-1</sup> due to -CH<sub>3</sub> symmetric stretching and -CH<sub>2</sub> asymmetric stretching while the band at 1380 cm<sup>-1</sup> appeared due to -CH bending. The peaks of Amide I bands (two types of hydrogen bonds between C=O group with the -NH group of the adjacent chain and the -OH group of the inter-chain) have been observed at 1629 and 1662 cm<sup>-1</sup>. Amide II band (in-plane N–H bending and C–N stretching mode) has been observed at 1558 cm<sup>-1</sup>. The peaks ranging from 1027 to 1163 cm<sup>-1</sup> can be attributed to the asymmetric bridge oxygen and C–O stretching<sup>22</sup>. After impregnation with Sn(VI), the -OH peak gets broadened due to alterations in hydrogen bonding network of chitin (Fig.1b). In SnC, the peak at 813 cm<sup>-1</sup> is assigned to Sn-O vibration. Small peaks between 1600 cm<sup>-1</sup>– 1900 cm<sup>-1</sup> are attributed to Sn-OH vibrational modes<sup>23</sup>. The changes in IR spectra of chitin confirmed that tin was impregnated on chitin matrix.

In the XRD pattern of pure chitin (Fig 2a), the peak at  $2\theta = 19.6^\circ$  represents the (110) crystalline plane of chitin, together with a few other weak intensity peaks<sup>24</sup>. Sharp diffraction peaks between  $2\theta = 16^\circ$  and  $22^\circ$  values indicate that chitin has crystalline structure. The insolubility of chitin in water is due to its rigid crystalline structure resulting from the regular formation of intra and intermolecular hydrogen bonds.

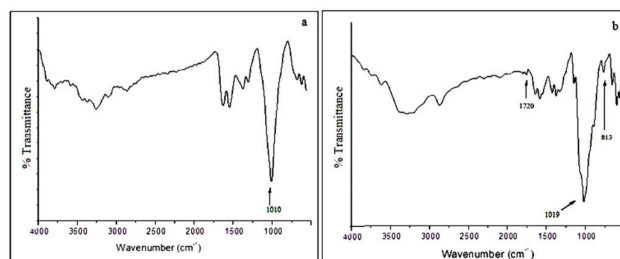


Fig.1 FT-IR spectrum of (a) Chitin (b) SnC.

In SnC (Fig.2b), the diffraction peaks at  $2\theta = 26.5^\circ$  and  $51.5^\circ$  for the (110) and (211) planes of Sn (JCPDS 21-1250) confirm impregnation of tin on chitin<sup>25</sup>. After adsorption of fluoride, (Fig.2c), the decrease in intensity of peaks at  $2\theta = 26.5^\circ$  and  $51.5^\circ$  indicate deterioration of crystallinity due to interaction between Sn(IV) and fluoride ion.

The SEM images (Fig 3) clearly show structural and morphological differences in chitin, SnC and fluoride-adsorbed SnC. The chitin seems to have a smooth surface morphology. But the SnC shows porous and rough morphology due to the impregnation of Sn(IV) thereby increasing the surface area and porosity. In the EDX spectrum of SnC, a peak of Sn appeared in the range 3 to 4 eV confirmed the successful loading of Sn onto the chitin matrix. The adsorption of fluoride was ascertained from the EDX spectrum which shows the presence of fluorine along with the other major peaks such as C, O, N and Sn respectively.

#### Thermal analysis

In the thermogram of chitin (Fig. 4a), two decomposition steps could be observed, the first occurs in the range of  $50\text{--}110^\circ\text{C}$ , and is attributed to water evaporation. The second occurs in the range of  $300\text{--}400^\circ\text{C}$  and could be attributed to the degradation of the polysaccharide structure of the molecule, including the dehydration of polysaccharide rings and the decomposition of the acetylated and deacetylated units of chitin<sup>26</sup>.

TGA curve of SnC also shows weight losses in the same regions. However, the percent weight loss has been reduced substantially from 55% to 18%. This indicates better thermal stability of SnC over chitin that can be attributed to incorporation of metal ion into the matrix leading to crosslinking of the polymeric chains. As the tin metal is much more stable as compared to organic polymer, it imparts additional stability to the matrix.

The DTA curve for chitin shows two endotherms. The one around  $90^\circ\text{C}$  can be attributed to removal of moisture while the one at  $380^\circ\text{C}$  that overlays the exotherm at  $400^\circ\text{C}$  indicates the decomposition. In case of SnC, the exothermic peak around  $400^\circ\text{C}$  indicates partial breakdown of polymeric or crosslinked structure.

The surface area is a vital parameter in adsorption study. BET surface area and pore volume of chitin and SnC were measured by nitrogen adsorption-desorption method at 77 K. From Table 1, it is clear that the surface area and pore volume of SnC is higher than that of chitin. The increase in surface area and pore volume of SnC is attributed to interaction between Sn and chitin as observed in SEM images. It leads to formation

of porous structure thereby enhancing the surface area as well as pore volume.

#### Effect of contact time

The effect of contact time on the efficiency of defluoridation by SnC was studied by varying the contact time in the range 5-75 min with initial fluoride concentration of 5, 10 and 15 mg/L with 100 mg SnC at 298 K. The adsorption was found to be rapid initially and reached equilibrium in about 45 min (Fig. 5a). This is quite obvious because of availability of more adsorption sites on SnC surface in the beginning which consequently get loaded with fluoride ions with time.

#### Effect of adsorbent dose

The dosage of SnC for defluoridation from aqueous medium was determined by varying the amount from 20 mg to 200 mg with initial fluoride concentration of 5, 10 and 15 mg/L for contact time of 45 min. It can be seen from the results (Fig. 5b) that, beyond 100 mg of SnC dose, the adsorption-desorption equilibrium is reached resulting in no observable rise in % removal of fluoride. Hence, 100 mg of SnC was fixed as the optimal dosage in all subsequent experiments.

#### pH point of zero charge ( $\text{pH}_{\text{PZC}}$ )

The pH at the point of zero charge ( $\text{pH}_{\text{PZC}}$ ) of the adsorbent was determined by batch equilibration technique<sup>27</sup>. In eight conical flasks, 50 mL of 0.1M NaCl solution were taken and 100 mg of SnC adsorbent was added to each flask. The initial pH was adjusted from 2.0 to 9.0 using dilute  $\text{H}_2\text{SO}_4$  and NaOH solutions. After a period of 24 h, the final pH values of supernatant solutions were measured. The  $\text{pH}_{\text{PZC}}$  of the SnC adsorbent was determined from the plot of  $\Delta\text{pH}$  [ $\text{pH}_{\text{initial}} - \text{pH}_{\text{final}}$ ] versus  $\text{pH}_{\text{initial}}$ . The  $\text{pH}_{\text{PZC}}$  was found to be 4.8 (Fig.5c). When  $\text{pH} < \text{pH}_{\text{PZC}}$  the surface charge would be positive, and at  $\text{pH} > \text{pH}_{\text{PZC}}$ , it would be negative. Therefore, the positive adsorbent surface favours the adsorption of fluoride, whereas above  $\text{pH}_{\text{PZC}}$ , the fluoride would be adsorbed to a lesser extent due to the repulsive interaction between fluoride ions and negative adsorbent surface.

**Table 1** Surface parameters

Material	Surface Area ( $\text{m}^2/\text{g}$ )	Pore volume ( $\text{cm}^3/\text{g}$ )
Chitin	1.78	$6.0 \times 10^{-3}$
SnC	2.83	$30.1 \times 10^{-3}$

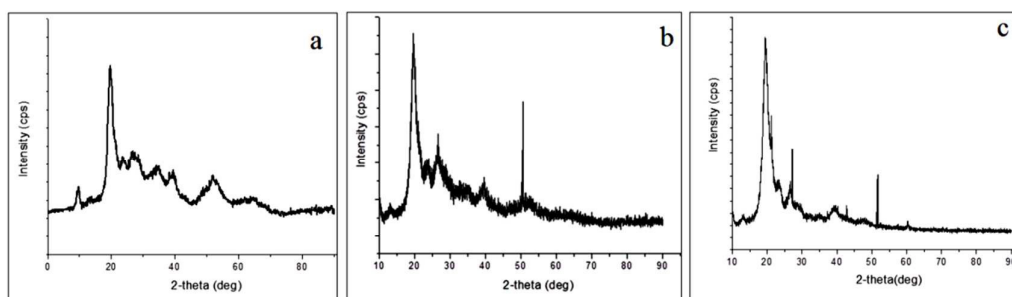


Fig.2 XRD pattern (a) Chitin (b) SnC (c) After adsorption of  $F^-$ .

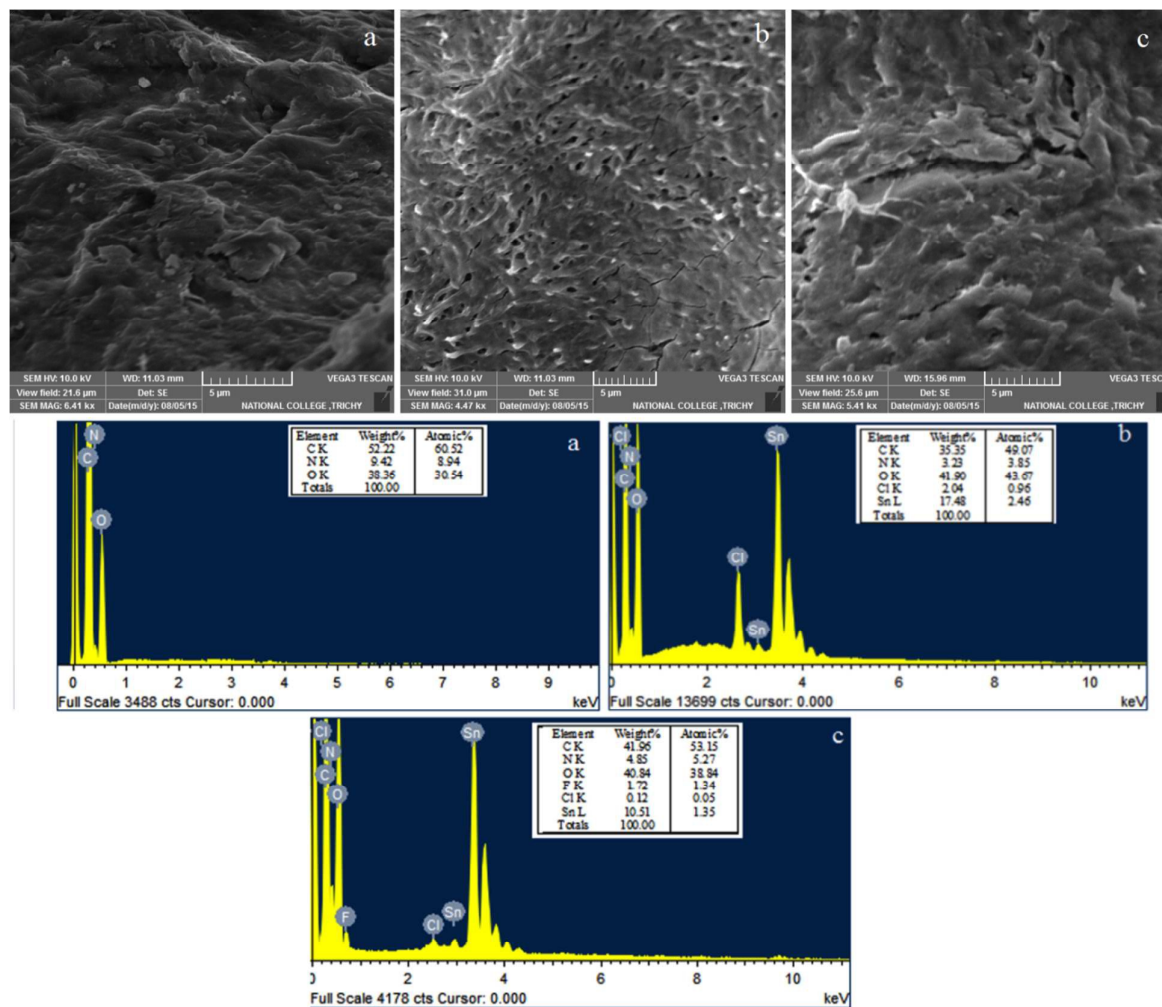


Fig.3 SEM Images and EDX spectrum (a) Chitin (b) SnC (c) After adsorption of  $F^-$ .

### Effect of pH

At low pH, the formation of undissociated HF attributes to reduction in the defluoridation. Also, the small size of fluoride ion leads to higher degree of solvation<sup>28</sup>. The pH of the solution was varied from 2.0 to 8.0 at varying initial fluoride ion concentration of 5, 10 and 15 mg/L, contact time of 45 min at room temperature. The effect of pH onto SnC biopolymer

adsorbent for the fluoride ion adsorption has been shown in Fig.5d. It was found that defluoridation was maximum at pH 4.0 and so the pH of  $4.0 \pm 0.2$  was maintained throughout the studies.

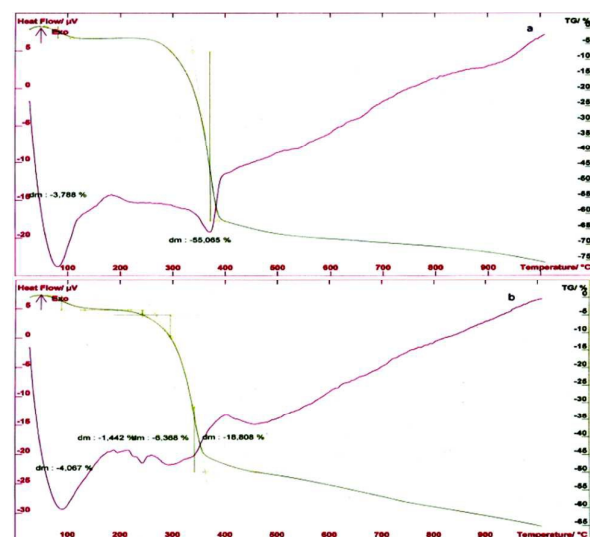


Fig. 4 TGA-DTA analysis (a) Chitin (b) SnC.

### Adsorption isotherms

To quantify the sorption capacity of SnC for fluoride sorption, Langmuir and Freundlich isotherms have been studied at three different temperatures (303, 313 and 323K). The adsorption studies were carried out by equilibrating 50 mL aqueous solutions of varying initial fluoride concentrations (5 to 70 mg/L) at optimized pH 4.0 and adsorbent dose of 100 mg for 45 min.

### Langmuir isotherm

The monolayer adsorption on homogeneous surface can be illustrated by Langmuir isotherm model<sup>29</sup>. It relates the maximum adsorption capacity ( $q_0$ ) and the Langmuir constant related to affinity of binding sites ( $b$ ) in linearized Langmuir equation-

$$\frac{C_e}{q_e} = \frac{1}{q_0 b} + \frac{C_e}{q_0} \quad (3)$$

The maximum adsorption capacity  $q_0$ , and the constant  $b$  were obtained from the slope and intercept of the plot of  $C_e/q_e$  against  $C_e$  (Fig 6a). A high defluoridation capacity of 14.77 mg/g at 323 K accounts for excellent adsorption behavior of SnC for fluoride. A dimensionless separation factor  $R_L$  that describes the feasibility of the sorption phenomenon is given by-

$$R_L = \frac{1}{1 + bC_0} \quad (4)$$

The value of  $R_L$  was found to be less than unity (Table. 2) indicating the effective interaction<sup>30</sup> between the Sn-chitin and fluoride.

### Freundlich isotherm

A linearized Freundlich isotherm<sup>31</sup> equation for aqueous solutions is given as

$$\log q_e = \log k_f + \frac{1}{n} \log C_e \quad (5)$$

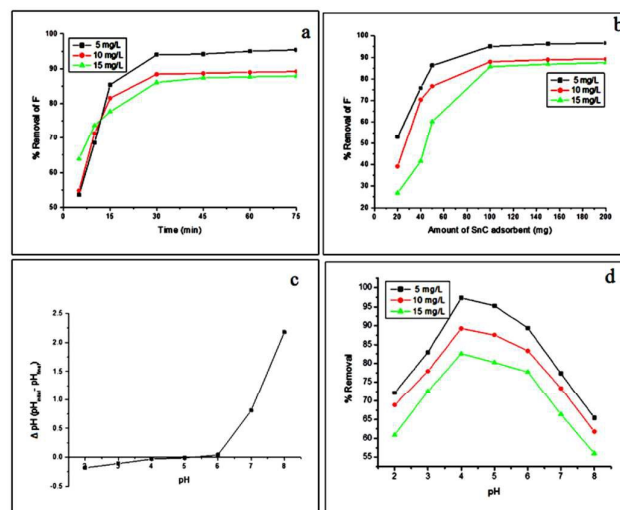


Fig.5 Effect of (a) Contact time (b) Adsorbent dose (c) Point of zero charge and (d) pH on adsorption efficiency.

Where  $k_f$  refers to adsorption capacity and  $n$  indicates the adsorption intensity. The logarithmic plot of  $q_e$  against  $C_e$  gives the constants  $k_f$  and  $n$  (Fig.6b). The smaller value of  $1/n$  (higher value of  $n$  between 1 and 10) signifies an active interaction<sup>32</sup> between SnC and fluoride.

### Chi square analysis

To identify a suitable isotherm model for the sorption of fluoride on SnC, chi-square analysis<sup>33</sup> has been carried out. The mathematical statement is given by

$$\chi^2 = \sum \frac{(q_e - q_{e,m})^2}{q_{e,m}} \quad (6)$$

The value of  $\chi^2$  would be less when the data obtained from a particular isotherm model is close to the experimental values. The results of chi-square test are shown in Table. 2. The lower  $\chi^2$  values for Freundlich isotherm as compared to Langmuir isotherm suggests that Freundlich model is the best fitting model for the fluoride removal by SnC. Similar result has been obtained from the plot of  $q_e$  versus  $C_e$  (Supplementary Fig.1)

Table 2 Study of isotherm models

Sl. No.	Isotherm	Parameters	303K	313K	323K
1	Langmuir	$q_0$ (mg/g)	12.47	13.44	14.77
		$b$ (L/mg)	0.16	0.09	0.06
		$R_L$	0.12	0.21	0.35
		$r^2$	0.941	0.903	0.887
		$\chi^2$	0.013	0.014	0.079
2	Freundlich	$K_f$ (mg <sup>1-1/n</sup> /g/L)	2.20	1.67	1.14
		$n$	2.03	1.84	1.60
		$r^2$	0.998	0.989	0.984
		$\chi^2$	9.63E-07	0.006	0.005

### Kinetics of adsorption

The amount of metal ion adsorbed by the adsorbent depends on the contact time and thus, the study of the kinetics of adsorption is of considerable significance. The studies were carried out using three different fluoride concentrations at optimized pH 4.0. A 50 ml fluoride solution was equilibrated with 100 mg of adsorbent at three different temperatures for different time intervals (5-90min). The results obtained have been summarized in Table 3.

The pseudo-first-order and pseudo-second-order kinetic models were employed to correlate the solid-liquid adsorption. The pseudo-first-order kinetics<sup>34</sup> is given by the equation

$$\log(q_e - q_t) = \log q_e - \frac{k_1 t}{2.303} \quad (8)$$

where  $q_e$  (mg /g) and  $q_t$  (mg /g) refer to the amounts of fluoride adsorbed at equilibrium and at time  $t$  with the first-order rate constant  $k_1$  ( $\text{min}^{-1}$ ). The plot of  $\log(q_e - q_t)$  against  $t$  gives pseudo-first-order rate constant. (Supplementary Fig. 2)

The pseudo-second-order equation<sup>35</sup> is given as

$$\frac{t}{q_t} = \frac{1}{k_2 q_e^2} + \frac{t}{q_e} \quad (9)$$

where  $k_2$  is the pseudo-second-order rate constant in  $\text{g/mg}/\text{min}$ . The plot of  $\log t/q_t$  against  $t$  (Supplementary Fig. 3) gives pseudo-second-order rate constant. Regression coefficient of 0.999 for pseudo-second-order rate kinetics offers a best fit model in adsorption of fluoride by SnC.

Permeation of fluoride by diffusion from bulk liquid phase to the surface of the adsorbent is rate determining step as explained by Weber Morris intraparticle diffusion model<sup>36</sup>. According to this model,  $q_t$  and  $t^{1/2}$  of adsorption process are related as:

$$q_t = k_{\text{int}} \cdot t^{1/2} + C \quad (10)$$

If the intercept in plot of  $q_t$  versus  $t^{1/2}$  passes through origin, then intraparticle diffusion is the only rate-limiting step. This plot is linear and the slope gives the intraparticle rate constant  $k_{\text{int}}$  in  $\text{mg}/\text{g}/\text{min}^{1/2}$ . The non-zero intercept (Supplementary Fig. 4) showed that diffusion is not the only rate-limiting step

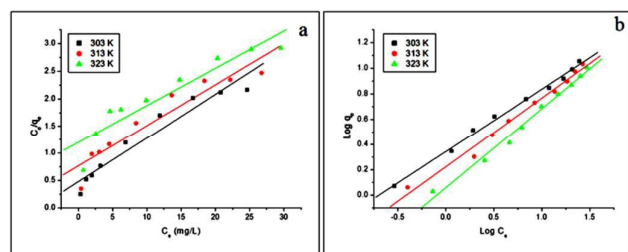


**Fig. 6** (a) Langmuir adsorption isotherm (b) Freundlich adsorption isotherm.

indicating that the adsorption of fluoride by SnC was controlled by boundary layer as well as diffusion process<sup>37</sup>.

### Thermodynamics of adsorption

Effect of temperature on adsorption of fluoride by SnC was studied in order to obtain relevant thermodynamic parameters with three different initial fluoride concentrations. The obtained results are depicted in Table 4.

The free energy change of adsorption ( $\Delta G^0$ ) is given by

$$\Delta G^0 = -RT \ln K \quad (11)$$

and van't Hoff equation<sup>38</sup> which relates standard entropy ( $\Delta S^0$ ) and enthalpy ( $\Delta H^0$ ) changes is given by

$$\ln K = \frac{\Delta S^0}{R} - \frac{\Delta H^0}{RT} \quad (12)$$

where  $R$  is the gas constant ( $8.314 \text{ J/mol}/\text{K}$ ). The value of equilibrium constant  $K$  has been evaluated from the ratio of concentration of fluoride adsorbed to that in the solution phase. The values of  $\Delta H$  ( $\text{kJ/mol}$ ) and  $\Delta S$  ( $\text{kJ/mol}/\text{K}$ ) were obtained from slope and intercept of the plot of  $\ln K$  against  $1/T$  respectively (Fig.7). The negative value of standard free energy change  $\Delta G^0$  indicates the spontaneous nature; negative enthalpy change indicates the exothermic nature while negative entropy change indicates the decrease in randomness of fluoride as it passes from solution to adsorbed state.

### Column study

In order to understand the applicability of adsorbent for larger sample volumes, column adsorption studies were performed using polypropylene column (30 cm length, 1 cm inner diameter) packed with 1 g of adsorbent to the height of 6 cm. Fluoride solution (10 and 15 mg /L) maintain at pH 4.0 were passed through the column at a flow rate of 5 mL/min. After every 10 min interval, solution phase concentration of fluoride was analyzed in column eluate. The important parameters obtained from breakthrough curve (Fig. 8a) are calculated using following formulae and results were depicted in Table 5. These results clearly indicate that larger sample volumes containing fluoride can be effectively treated using column method compared to batch adsorption.

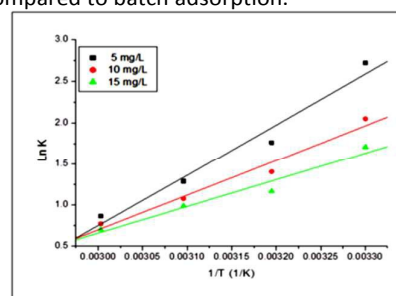


**Fig. 7** van't Hoff plots.

**Table 3** Kinetics of adsorption of fluoride on SnC.

Temperature (K)	Rate model	Parameters	Concentrations		
			5 (mg/L)	10 (mg/L)	15 (mg/L)
303	Pseudo-first-order kinetics	$K_1$	0.11	0.12	0.11
		$q_e$ exp (mg/g)	1.18	2.22	3.26
		$q_e$ cal (mg/g)	0.51	1.06	0.74
		$r^2$	0.934	0.921	0.856
	Pseudo-second-order kinetics	$K_2$	0.23	0.13	0.16
		$q_e$ exp (mg/g)	1.18	2.22	3.26
		$q_e$ cal (mg/g)	1.26	2.35	3.38
		$r^2$	0.998	0.999	0.998
	Intraparticle diffusion	$K_{int}$	0.08	0.14	0.14
$r^2$		0.861	0.908	0.872	
313	Pseudo-first-order kinetics	$K_1$	0.11	0.03	0.12
		$q_e$ exp (mg/g)	1.15	2.00	2.99
		$q_e$ cal (mg/g)	0.62	0.91	1.11
		$r^2$	0.932	0.871	0.925
	Pseudo-second-order kinetics	$K_2$	0.16	0.09	0.14
		$q_e$ exp (mg/g)	1.15	2.00	2.99
		$q_e$ cal (mg/g)	1.26	2.19	3.12
		$r^2$	0.997	0.995	0.992
	Intraparticle diffusion	$K_{int}$	0.09	0.16	0.14
$r^2$		0.880	0.892	0.922	
323	Pseudo-first-order kinetics	$K_1$	0.11	0.11	0.12
		$q_e$ exp (mg/g)	1.07	1.86	2.85
		$q_e$ cal (mg/g)	0.85	0.78	0.98
		$r^2$	0.944	0.931	0.891
	Pseudo-second-order kinetics	$K_2$	0.17	0.23	0.19
		$q_e$ exp (mg/g)	1.07	1.86	2.85
		$q_e$ cal (mg/g)	1.24	1.97	2.96
		$r^2$	0.998	0.995	0.994
	Intraparticle diffusion	$K_{int}$	0.11	0.11	0.11
$r^2$		0.898	0.873	0.912	

$$\text{Breakthrough Capacity } \left(\frac{\text{mg}}{\text{g}}\right) = \frac{\text{Breakthrough Volume(L)} \times \text{Inlet concentration(mg/L)}}{\text{Wt. of adsorbent (g)}} \quad (12)$$

$$\text{Exhaustion Capacity} = \frac{\text{Exhaustion Volume(L)} \times \text{Inlet concentration(mg/L)}}{\text{Wt. of adsorbent (g)}} \quad (13)$$

$$\text{Degree of column utilization} = \frac{\text{Breakthrough Volume}}{\text{Exhaustion Volume}} \times 100 \quad (14)$$

The column eluent was tested for possible leaching of tin in the form of Sn(II) or Sn(VI). It was observed that such leaching does not take place under experimental conditions. However, it was found to contain significant concentration of chloride confirming the ion exchange phenomenon between fluoride and adsorbent.

#### Effect of assorted ions

The effect of co-anions on defluoridation capacity of SnC was studied with fixed initial concentration of 1mM for co-anions such as  $\text{SO}_4^{2-}$ ,  $\text{Cl}^-$ ,  $\text{NO}_3^-$ ,  $\text{CO}_3^{2-}$  and equivalent initial fluoride

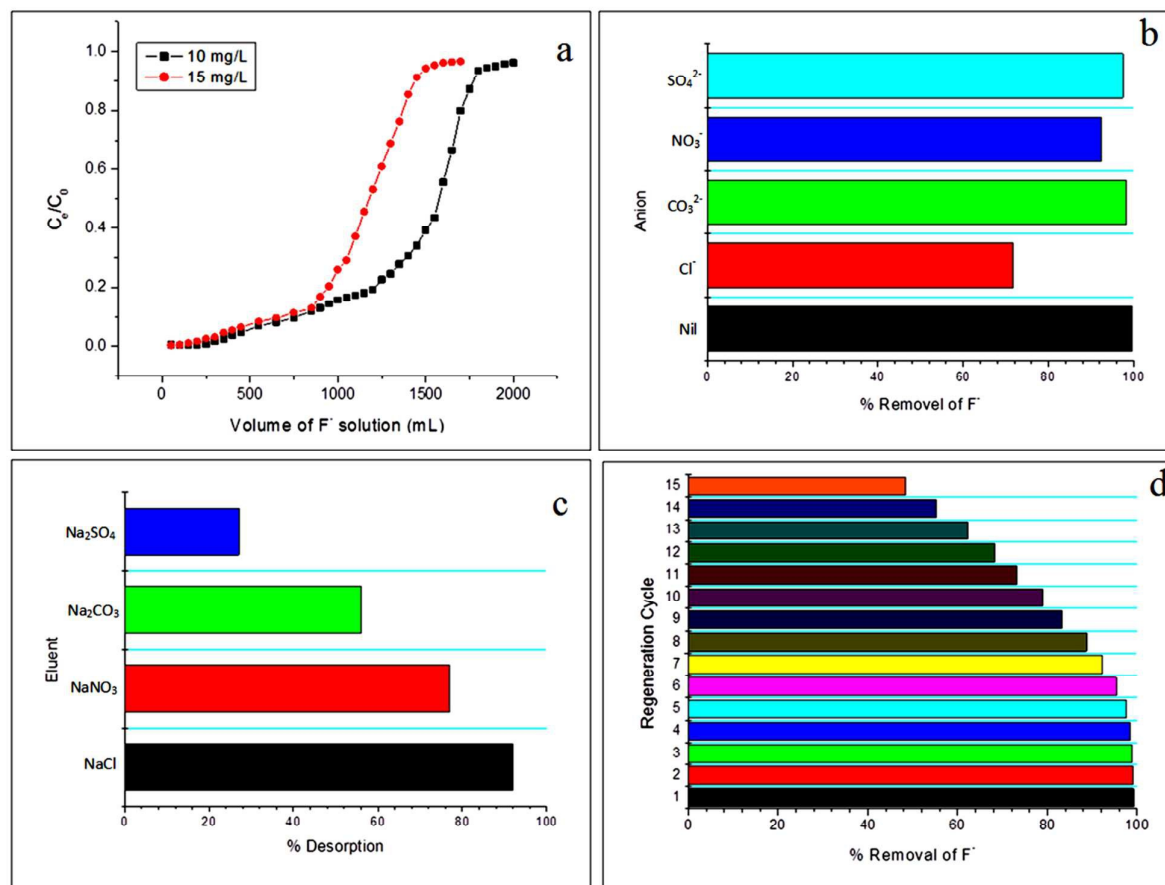
concentration. It is observed from Fig. 8b that presence of co-anions leads to decrease in defluoridation capacity due to the competition among them for the active sites on the adsorbent surface which depends on the charge, concentration and size of the anions<sup>39</sup>. Chloride ions have been found to be strongest interference.

#### Reusability of adsorbent

The regeneration of adsorbent is an important aspect from a greener point of view. Reagents such as sodium chloride, sodium nitrate, sodium sulphate and sodium carbonate were examined for desorption studies. The best results were obtained with 5% (v/v) sodium chloride solution. The NaCl solution results into waning of electrostatic interaction between SnC and fluoride ions leading to desorption of fluoride ions. From Fig.8c, it is observed that ionic salts such as NaCl and  $\text{NaNO}_3$  solutions shows good result for desorption of fluoride ion. The regenerated SnC were recharacterized by FT-IR and SEM-EDX indicating no structural changes in SnC. The regenerated SnC was tested for fifteen adsorption-desorption cycles and it was observed (Fig 8d) that there is marginal

**Table 4** Thermodynamic parameters of adsorption

Concentration (mg/L)	Parameter	T (K)				$\Delta H^0$ (kJ/mol)	$\Delta S^0$ (kJ/mol/K)
		303	313	323	328		
5	K	15.13	5.85	3.63	2.38	-50.82	-0.14
	$\Delta G^0$ (kJ/mol)	-6.84	-4.59	-3.46	-2.39		
10	K	7.77	4.07	2.93	2.16	-35.08	-0.09
	$\Delta G^0$ (kJ/mol)	-5.16	-3.66	-2.90	-2.14		
15	K	6.78	3.91	3.16	2.54	-27.06	-0.07
	$\Delta G^0$ (kJ/mol)	-4.31	-3.03	-2.65	-1.94		

**Fig. 8** (a) Effect of sample volume on column efficiency (b) Effect of co-anions (c) Effect of various reagents on desorption of loaded fluoride ion (d) adsorption cycles for regenerated SnC**Table 5** Column study: Parameters obtained from breakthrough curve

Inlet F <sup>-</sup> concentration (mg/L)	10	15
Breakthrough volume (mL)	800	600
Exhaustion volume (mL)	1750	1250
Breakthrough Capacity (mg/g)	8.0	9.0
Exhaustion Capacity (mg/g)	17.5	18.75
Degree of column utilization (%)	45.7	48.0

decrease in adsorption efficiency upto five cycles. However, the adsorption efficiency decreases substantially and remains only 48% in fifteenth cycle.

#### Fluoride sorption mechanism

The binding of  $\text{SnCl}_4$  on chitin can be explained by means of molecular binding to the surface of chitin containing hydroxyl groups as well as glycosidic linkages of chitin biopolymer<sup>40</sup>. The metal ion present on SnC adsorbent can interact with the fluoride ions in two ways. It has a strong electrostatic attraction with fluoride ions and also can exchange chloride ions with fluoride ions (Fig.9) resulting into an increase in adsorption capacity. The ion exchange phenomenon was confirmed by performing test for chloride ions in the supernatant obtained after fluoride adsorption on SnC and the eluate in column studies. The presence of chloride ions on SnC was also detected in EDX spectra of adsorbent. The EDX spectra clearly shows reduction in chloride peak with the introduction of fluoride peak after equilibration with fluoride. Apart from this, the hydrogen bonding between the chitin polymeric chains may also reinforce the adsorption of fluoride anion on the SnC.

#### Field Study

In order to confirm the applicability of the SnC for removal of fluoride, it was tested with sample taken from Chandrapur district which is fluoride affected area in Central India. The report of Central Ground Water Board, Nagpur region mentions about fluoride concentrations above maximum permissible limits in Chandrapur district. About 100 mg sorbent was added to 50 ml of fluoride containing water sample collected from Chandrapur region and kept for constant stirring at room temperature for 45 minutes. The results obtained for single adsorption are depicted in Table 6 demonstrating the ability of this material towards defluoridation.

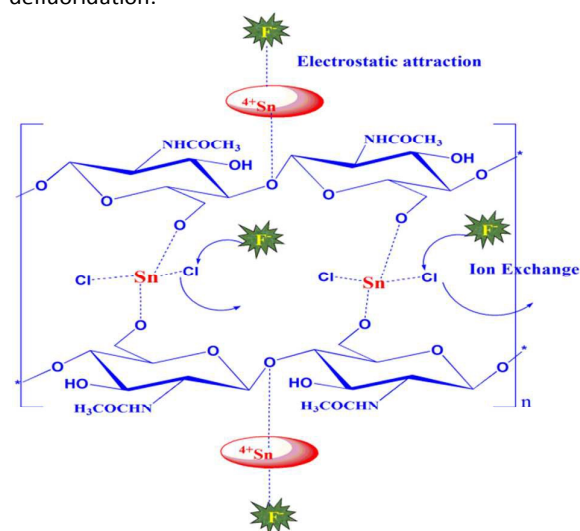


**Fig.9** Mechanism of fluoride adsorption on SnC

#### Comparison with other related adsorbents

Present work has been compared with similar studies carried out by various workers (Table 7) including the types of isotherm models studied, thermodynamic and kinetic studies, optimum pH and adsorption capacity under optimum conditions. The results clearly indicate that the adsorption capacity of SnC is higher than most of the reported materials except Zr(VI)-ethylene diamine. However, this material is obtained in the form of gel which makes the separation difficult. The method is laborious and requires multiple decantations for fluoride removal. On the other hand, SnC method is a single extraction process. Another important advantage of SnC is the biodegradability of chitin that adds greener dimension.

#### Conclusions

Chitin was incorporated with Sn(VI) to give an excellent fluoride adsorbent SnC. Characterization of this material showed improved properties for better adsorption that led to adsorption capacity of 14.77 mg/g. The kinetics and isotherm studies indicate pseudo-second order kinetics in accordance with Freundlich adsorption isotherm. Column studies clearly indicated that the material can be used to larger sample volumes in column extraction as compared to batch extraction. Applicability towards real sample, recycling and reusability are the most encouraging properties of SnC.

#### Acknowledgements

The authors are thankful to RTM Nagpur University for University Research Project and Innovative Research Scheme.

**Table 6** Field trial results of the SnC.

Parameter	Before Treatment	After Treatment
$\text{F}^-$ (mg/L)	2.51	0.11
pH	7.51	7.43
$\text{SO}_4^{2-}$ (mg/L)	133.38	109.71
$\text{Cl}^-$ (mg/L)	247.75	152.32
Total hardness (mg/L)	382.21	241.74
Total dissolved solids (mg/L)	629.63	479.55

**Table 7** Comparison of SnC with reported adsorbents

Adsorbent	$q_e$	Study	pH	Kinetic model	thermodynamics	Mechanism	Iso-therm	Adsorbent characterization	Ref.
Nano-hydroxyapatite/chitin composite	2.84	E,K,T	3.0	Pseudo second order	Spontaneous and endothermic	Chemisorptions and ion exchange	L,F	SEM, EDX,FTIR	41
Lanthanum incorporated chitosan beads	4.7	E,K,T	5.0	Pseudo first order	Spontaneous and endothermic	Ion exchange	L,F	SEM, EDX,FTIR, XRD	13
Al-Zr impregnated cellulose	5.76	E,K,T	5.5	Pseudo second order	Spontaneous and exothermic	Electrostatic, hydrogen bonding and complexation	L,F	SEM, EDX,FTIR, XRD	40
Fe-Sn bimetal oxide	10.50	E,K,T	6.4	Pseudo second order	Non-spontaneous and endothermic	Ion exchange	L,F,D-R	SEM,FTIR, XRD	21
Zirconium impregnated cellulose	4.95	E,K,T	5.0	Pseudo second order	Spontaneous and exothermic	electrostatic	L,F,D-R, Tm	EDX,FTIR, XRD	42
Zr(IV) ethylenediamine	37.03	E,K,T	7.0	Pseudo second order	Spontaneous and endothermic	Electrostatic and ion exchange	L,F,D-R, Tm	SEM,FTIR, TGA-DTA	9
Sn impregnated chitin	14.77	E,K,T	4.0	Pseudo second order	Spontaneous and exothermic	Electrostatic and ion exchange	L,F	SEM-EDX,FTIR, TGA-DTA	This work

$q_e$ - Adsorption capacity E-equilibrium; K-kinetic; T-thermodynamic; L-Langmuir; F-Freundlich; D-R-Dubinin-Radushkevich; Tm-Temkin isotherms; X-ray diffraction (XRD); scanning electron microscopy(SEM); scanning electron microscopy coupled with energy dispersive X-ray spectroscopy (SEM-EDX); Fourier transform infrared spectroscopy (FT-IR), thermogravimetric analysis (TGA).

## References

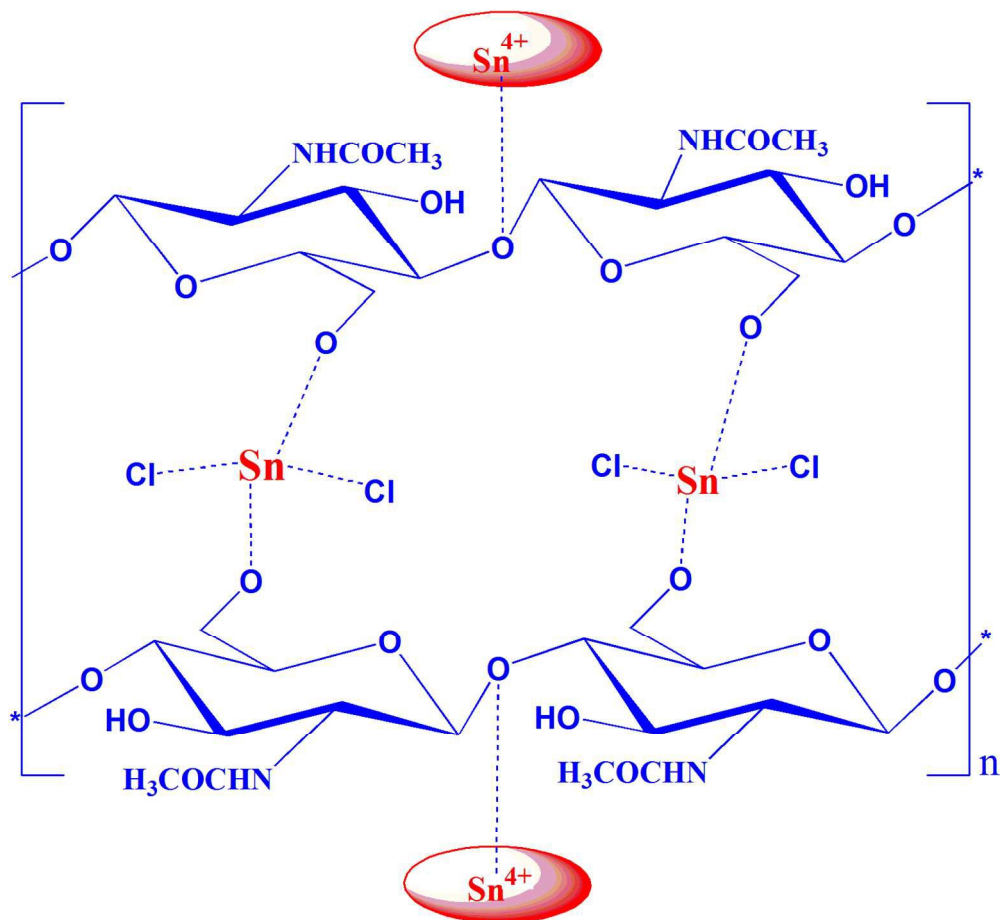
1. WHO Report, 1984. *Fluoride and Fluorides: Environment Health Criteria*. World Health Organisation.
2. V.T. Yadugiri, *Curr. Sci.*, 2011, **100**, 1475–1477.
3. J. Fawell, K. Bailey, E. Chilton, E. Dahi, L. Fewtrell, Y. Magara, *Fluoride in Drinking Water*, World Health Organization, IWA Publishing, UK, 2006.
4. R.C. Meenakshi, Maheshwari, Fluoride in drinking water and its removal, *J. Hazard. Mater.* B137 (2006) 456–463.
5. G.M. Whiteford, *J. Dent. Res.* 1990, **69**, 539–549.
6. M. Amini, K. Mueller, K.C. Abbaspour, T. Rosenberg, M. Afyuni, K.N. Møller, M. Sarr, C.A. Johnson, *Environ. Sci. Technol.*, 2008, **42**, 3662–3668.
7. S. Ayoob, A.K. Gupta, *Crit. Rev. Environ. Sci. Technol.*, 2006, **36**, 433–487.
8. S. Jagtap, M.K. Yenkie, N. Labhsetwar, S. Rayalu, *Chem Rev.* 2012, **112**, 2454–66.
9. S.K. Swain, S. Mishra, T. Patnaik, R.K. Patel, U. Jha, R.K. Dey, *Chem. Eng. J.*, 2012, **184**, 72–81.
10. S.K. Swain, T. Patnaik, P.C. Patnaik, U. Jha, R.K. Dey, *Chem. Eng. J.*, 2013, **215–216**, 763–771.
11. X.P. Liao, B.I. Shi, *Environ. Sci. Technol.*, 2005, **39**, 4628–4632.
12. C. Janardhana, G. Nageswararao, R. Saisatish, P. Sunil Kumar, V. Anil Kumar, M. Vijaymadhav, *Indian J. Chem. Technol.*, 2007, **14**, 350–354.
13. A. Bansawal, D. Thakre, N. Labhsetwar, S. Meshram, S. Rayalua, *Colloids Surf. B Biointerfaces.*, 2009, **74**, 216–224.
14. M. Vandebossche, M. Jimenez, M. Casetta, M. Traisnel, *Crit. Rev. Env. Sci. Tech.*, 2015, **45**, 1644–1704.
15. A. Bhatnagar, M. Sillanpaa, *Adv. Colloid Interface Sci.*, 2009, **152**, 26–38.
16. M. N. V Ravi Kumar, *React. Funct. Polym.*, 2000, **46**, 1–27.
17. P. N. Sudha, T. Gomathi, P.A. Vinodhini, K. Nasreen, Chapter Seven – Marine Carbohydrates of Wastewater Treatment, *Adv. Food Nutr. Res.*, 2014, **73**, 103–143.
18. Jose L. Davila-Rodriguez, Vladimir A. Escobar-Barrios, Jose R. Rangel-Mendez, *J. Fluorine Chem.*, 2012, **140**, 99–103.
19. Jose L. Davila-Rodriguez, Vladimir A. Escobar-Barrios, Keiko Shirai, Jose R. Rangel-Mendez, *J. Fluorine Chem.*, 2009, **130**, 718–726.
20. Sanjay P. Kamble, Sneha Jagtap, Nitin K. Labhsetwar, Dilip Thakare, Samuel Godfrey, Sukumar Devotta, Sadhana S. Rayalu, *Chem. Eng. J.*, 2007, **129**, 173–180.
21. Krishna Biswas, Kaushik Gupta, Uday Chand Ghosh, *Chem. Eng. J.*, 2009, **149**, 196–206.
22. Tsunenori Kameda, Mitsuhiro Miyazawa, Hiroshi Ono, Mitsuru Yoshida, *Macromol. Biosci.*, 2005, **5**, 103–106.
23. A.N. Banerjee, S. Kundoo, P. Saha, K.K. Chattopadhyay, *J. Sol-Gel Sci. Technol.*, 2003, **28**, 105–110.
24. Xi Chen, Shu Ling Chew, Francesca M. Kerton, Ning Yan, *Green Chem.*, 2014, **16**, 2204–2212.
25. N. Srivastava, M. Mukhopadhyay, *Ind. Eng. Chem. Res.*, 2014, **53**, 13971–13979.
26. R. Jayakumar, T. Egawa, T. Furuike, S.V. Nair, H. Tamura, *Polym. Eng. Sci.*, 2009, **49**, 844–849.
27. N.A. Oladoja, Y.D. Aliu, *J. Hazard. Mater.*, 2009, **164**, 1496–1502.
28. A.M. Raichur, M.J. Basu, *Sep. Purif. Technol.*, 2001, **24**, 121–127.
29. I. Langmuir, *J. Am. Chem. Soc.*, 1918, **40**, 1361–1403.
30. S. Kahu, D. Saravanan, R. Jugade, *Water Sci. Technol.*, 2014, **70**, 2047–2055.
31. H.M.F. Freundlich, *Z. Phys. Chem.*, 1906, **57**, 385–470.
32. A. Shekhawat, S. Kahu, D. Saravanan, R. Jugade, *Int. J. Biol. Macromol.*, 2015, **80**, 615–626.
33. N. Viswanathan, S. Meenakshi, *J. Hazard. Mater.*, 2010, **178**, 226–232.
34. S. Lagergren, *K. Sven. Vetenskapskad. Handl.*, 1898, **24**, 1–39.
35. L.M. Camacho, A. Torres, D. Saha, S. Deng, *J. Colloid Interface Sci.*, 2010, **349**, 307–331.
36. W.J. Weber, J.C. Morris, *J. Sanit. Eng. Div. Am. Soc. Civ. Eng.*, 1963, **89**, 3–60.
37. E. Bulut, M. Ozacar, I. A. Sengil, *Microporous Mesoporous Mater.*, 2008, **115**, 234–246.
38. A.M. Donia, A.A. Atia, H.A. El-Boraey, D. Mabrouk, *Sep. Purif. Technol.*, 2006, **49**, 64–70.
39. N. Viswanathan, S. Meenakshi, *J. Colloid Interface Sci.*, 2008, **322**, 375–383.
40. M. Barathi, A.S.K. Kumar, N. Rajesh, *J. Environ. Chem. Eng.*, 2013, **1**, 1325–1335.
41. C. S. Sundaram, N. Viswanathan, S. Meenakshi, *J. Hazard. Mater.*, 2009, **172**, 147–151.
42. M. Barathi, A.S.K. Kumar, N. Rajesh, *Ultrasonics Sonochemistry*, 2014, **21**, 1090–1099.

**RSC Advances**

ARTICLE

RSC Advances Accepted Manuscript

## GRAPHICAL ABSTRACT



136x134mm (300 x 300 DPI)